Multidetector CT and MR Imaging of Cardiac Tumors

Eun Young Kim, MD[1]
Yeon Hyeon Choe, MD[1]
Kiick Sung, MD[2]
Seung Woo Park, MD[3]
Ji Hye Kim, MD[1]
Young-Hyeh Ko, MD[4]

The purpose of this article is to provide a current review of the spectrum of multidetector CT (MDCT) and MRI findings for a variety of cardiac neoplasms. In the diagnosis of cardiac tumors, the use of MDCT and MRI can help differentiate benign from malignant masses. Especially, the use of MDCT is advantageous in providing anatomical information and MRI is useful for tissue characterization of cardiac masses. Knowledge of the characteristic MRI findings of benign cardiac tumors or thrombi can be helpful to avoid unnecessary surgical procedures. Presurgical assessment of malignant cardiac tumors with the use of MDCT and MRI may allow determination of the resectability of tumors and planning for the reconstruction of cardiac chambers.

Index terms:
Cardiac tumor
Magnetic resonance (MR)
Multidetector CT

DOI:10.3348/kjr.2009.10.2.164

Korean J Radiol 2009;10:164-175
Received May 2, 2008; accepted after revision August 26, 2008.

[1]Department of Radiology and Center for Imaging Science; [2]Department of Thoracic and Cardiovascular Surgery; [3]Division of Cardiology, Department of Medicine; [4]Department of Pathology, Samsung Medical Center, Sungkyunkwan University School of Medicine, Seoul 135-710, Korea

Address reprint requests to:
Yeon Hyeon Choe, MD, Department of Radiology and Center for Imaging Science, Samsung Medical Center, Sungkyunkwan University School of Medicine, 50 Irwon-dong, Gangnam-gu, Seoul 135-710, Korea.
Tel. (822) 3410-2509
Fax. (822) 3410-2559
e-mail: yhchoe@skku.edu

Cardiac tumors have a cumulative prevalence of 0.002–0.3% as determined from an autopsy (1). Primary cardiac neoplasms include both benign and malignant histological types (Table 1) (2). Metastatic involvement of the heart is approximately 30 times more prevalent than primary cardiac tumors. Although primary cardiac tumors are rare and the histological types are varied, familiarity with certain imaging features can help distinguish between benign and malignant cardiac tumors. Up to now, transthoracic echocardiography has been the most widely used imaging modality for the evaluation of cardiac masses. Echocardiography is the best imaging modality to depict small masses that arise from the cardiac valves. However, visualization of extracardiac extension is suboptimal with the use of transthoracic echocardiography for the evaluation of malignant cardiac masses. Although the use of transesophageal echocardiography overcomes the limited acoustic window of the transthoracic mode, the airways and lungs can be obstacles for imaging of the aortic arch, pulmonary arteries and some systemic and pulmonary veins (3).

MRI is presently the modality of choice to evaluate cardiac tumors. High contrast resolution and multiplanar capability allow a specific diagnosis and optimal evaluation of myocardial infiltration, pericardial involvement and extracardiac extension. Recently, multidetector CT (MDCT) has been increasingly utilized for cardiac imaging. The short image acquisition time for MDCT is advantageous in cardiac imaging as compared with the use of MRI. With the use of helical CT, gating the cardiac images to the electrocardiogram (ECG) can be accomplished either by scanning or reconstructing raw data at the point of the least cardiac motion (4). The use of ECG-gated MDCT has better soft tissue contrast than echocardiography and can definitively characterize fatty content and calcifications. A wide field-of-view with MDCT helps to assess the extent of a cardiac malignancy and helps to detect metastatic lesions. However, the

role of MDCT in the evaluation of cardiac tumors has not been described adequately in the literature. This article describes the imaging techniques of the use of MDCT and MRI for the evaluation of cardiac masses and the imaging features of benign and malignant cardiac tumors.

Multidetector CT Techniques

Volumetric data of entire hearts were obtained using a 64-slice MDCT scanner (Aquilion 64; Toshiba Medical Systems, Tokyo, Japan) with the administration of intravenous contrast material. With the use of a dual-syringe power injector (Stellant-Dual Flow; Medrad, Pittsburgh, PA), 65 mL of a nonionic contrast material (350 mg I/mL iomeprol; Bracco Imaging, Milan, Italy) was injected at a rate of 4 mL/s. The injection of contrast material was followed by injection of 30 mL of mixed normal saline and contrast medium (20% contrast medium and 80% normal saline) at 3 mL/s. A real time bolus tracking technique (SureStart; Toshiba Medical Systems, Tokyo, Japan) was used with a region of interest in the ascending aorta. A CT scan was started at a threshold value of 200 Hounsfield units (HU). Imaging was started from the aortic root to the caudal end of the heart. The CT scanning parameters were as follows: 120 kV, 400 mA, 64 $\times$ 0.5 mm collimation, at pitch values of 0.2–0.3 and a 0.4 second tube rotation time. ECG-gated dose modulation was applied according to the patient heart rate to reduce the radiation dose to patients. Raw data were reconstructed using retrospective ECG gating. The transverse images were reconstructed with a slice thickness of 0.4 mm and an image matrix of 512 $\times$ 512 pixels. A display field of 26 cm was sufficient, which corresponded to a pixel size of approximately 0.5 mm.

MR Imaging Techniques

A cardiac surface coil usually provided good signals with the use of a 1.5-T scanner (Achieva 1.5 T; Philips Medical Systems, Best, The Netherlands). Various pulse sequences were used for imaging cardiac tumors. ECG-gated double inversion-recovery images (TE = 10 msec), triple inversion-recovery images (TE = 100 msec), transverse or short-axial breath-hold cine MR images (balanced turbo field echo [TFE], TR/TE = 3.1/1.6 msec) were usually obtained before contrast injection. After injection of contrast material (0.1 mmol/kg at a rate of 2–3 mL/sec; Gd-diethylenetriamine-pentaacetic acid, Magnevist; Bayer Schering Pharma, Berlin, Germany), postcontrast images were obtained using either a double inversion-recovery sequence or delayed myocardial imaging (TFE, TR/TE = 4.5/1.4 msec) with suppression of the normal myocardial signals. Three-dimensional balanced TFE (TR/TE = 4.5/2.2 msec, slice thickness 2 mm, spacing 1 mm, 144 $\times$ 144 matrix) with respiratory gating was useful in depicting small masses in the cardiac valves or to detect thrombi. For visualization of ventricular thrombi, delayed myocardial imaging with a long inversion time of 400 msec could be used. To evaluate tumor vascularity, especially in hypervascular tumors such as hemangiomas, dynamic balanced TFE with sensitivity encoding was used for perfusion imaging.

BENIGN TUMORS

Myxomas

Myxomas are the most common benign tumor found in adults; these tumors present in adulthood between the fourth and seventh decades (5). The classic triad of

Table 1. Primary Tumors and Cysts of Heart and Pericardium

Type	Number (%)
Benign	
Myxoma	130 (24.2)
Lipoma	45 (8.4)
Papillary fibroelastoma	42 (7.9)
Rhabdomyoma	36 (6.8)
Fibroma	17 (3.2)
Hemangioma	15 (2.8)
Teratoma	14 (2.6)
Mesothelioma of atrioventricular node	12 (2.3)
Granular cell tumor	3
Neurofibroma	3
Lymphangioma	2
Subtotal	319 (59.8)
Pericardial cyst	82 (15.4)
Bronchogenic cyst	7 (1.3)
Subtotal	89 (16.7)
Malignant	
Angiosarcoma	39 (7.3)
Rhabdomyosarcoma	26 (4.9)
Mesothelioma	19 (3.6)
Fibrosarcoma	14 (2.6)
Malignant lymphoma	7 (1.3)
Extraskeletal osteosarcoma	5
Neurogenic sarcoma	4
Malignant teratoma	4
Thymoma	1
Leiomyosarcoma	1
Liposarcoma	1
Synovial sarcoma	1
Subtotal	125 (23.5)
Total	533 (100.0)

Note.— Adapted from McAllister and Fenoglio (2).

symptoms includes cardiac obstructive symptoms related to the obstruction of blood flow (Fig. 1), embolic events, and constitutional symptoms such as fever, malaise and weight loss. Thromboembolic events occur in 35% of left-sided myxomas to the brain, kidney, spleen and extremities and 10% of right-sided myxomas to the lung (5–7). Friable and gelatinous myxomas are more likely to embolize than firm and fibrous lesions (6). Approximately 75% of myxomas are found in the left atrium, typically, in the interatrial septum in the region of the fossa ovalis; 20% of myxomas are located in the right atrium, and rare cases are found in the ventricles. The use of contrast-enhanced CT usually demonstrates the presence of a well-defined spherical or ovoid intracavitary mass, which typically has lobular contours (Fig. 2). Tumor attenuation is lower than that of the unopacified blood. The intravenous administration of a contrast material helps better to define the lesion as a mass of low attenuation that is surrounded by enhancing intracardiac blood. Heterogeneity is a common feature of myxomas and is believed to reflect hemorrhage, necrosis, cyst formation, fibrosis or calcification. Myxomas tend to show markedly increased signal intensity as seen on the T2-weighted MR images (Fig. 3). However, myxomas can show areas of decreased signal intensity due to the presence of calcification or magnetic susceptibility artifacts caused by hemosiderin (8).

Lipomas

Lipomas are the second most common benign cardiac tumors encountered in adults (5), and these lesions have specific CT and MR imaging characteristics. The use of CT shows cardiac lipomas as homogeneous, low-attenuation masses either in a cardiac chamber or in the pericardial space (Fig. 4). MR imaging demonstrates lipomas to have homogeneous increased signal intensity as seen on the T1- and T2-weighted images that decreases with the use of fat-saturated sequences. As with soft-tissue lipomas, cardiac lipomas do not show enhancement with the administration

Fig. 1. Left atrial myxoma in 38-year-old female.
A. Reformatted ECG-gated multidetector CT image in 4-chamber view shows mass (arrow) in left atrium.
B. Note mass (arrow) extends into left ventricle during diastolic phase through mitral valve.

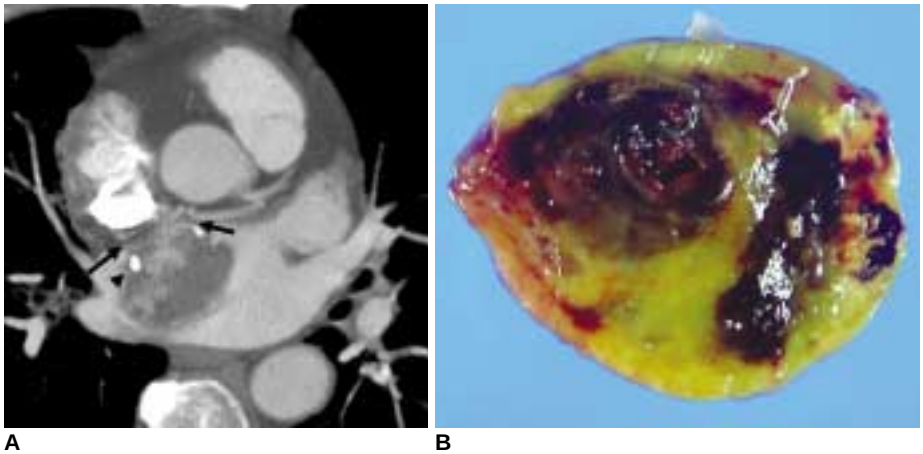

Fig. 2. Left atrial myxoma in 65-year-old male.
A. Reformatted ECG-gated multidetector CT image shows left atrial mass attached to interatrial septum by broad pedicle (arrows). Note strong contrast enhancement in part of mass with foci of calcification (arrowhead).
B. Gross specimen shows myxoid soft tissue mass with pale yellow and dark brown colors, which probably represent mixture of hemorrhage, necrosis, cyst formation and fibrosis.

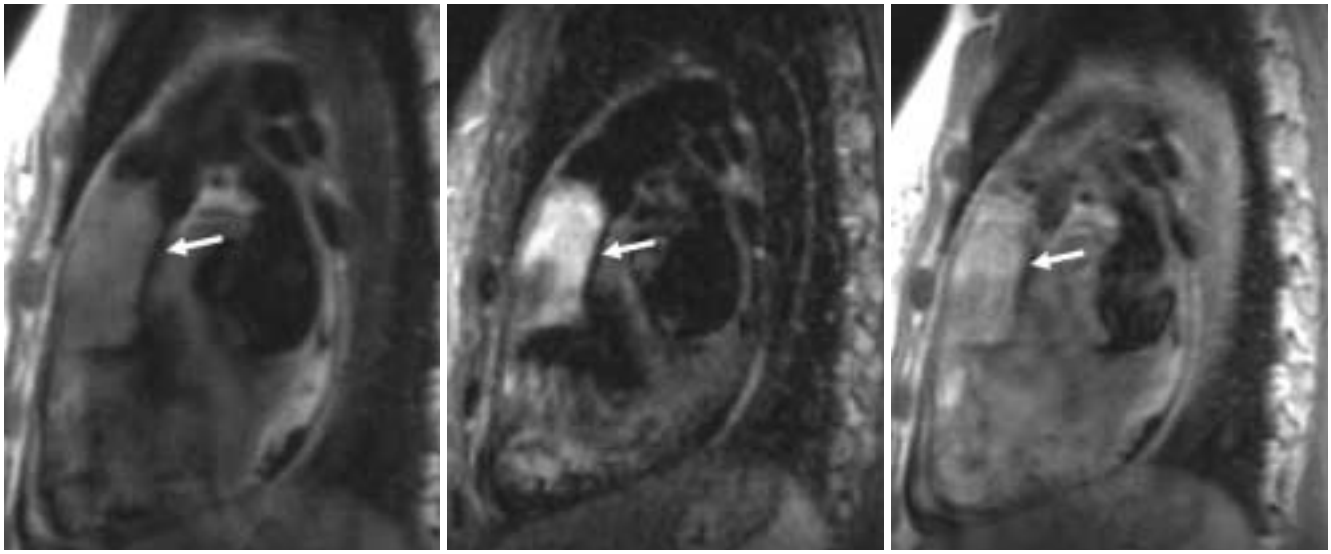

A B C

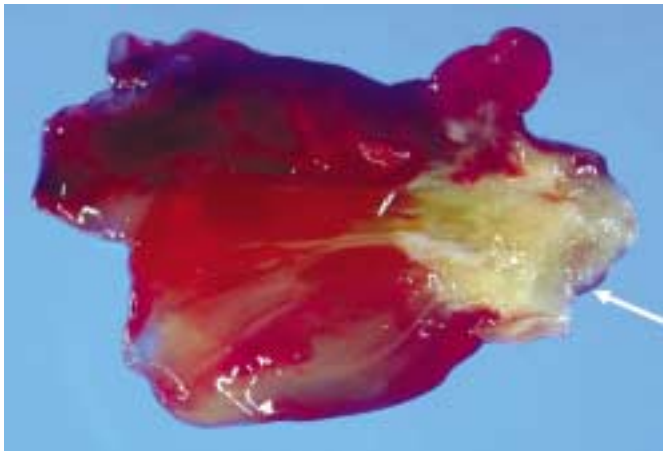

D

Fig. 3. Right ventricular myxoma in 30-year-old female.
A. Sagittal double inversion-recovery MR image demonstrates isointense mass (arrow) occupying right ventricular outflow tract.
B. Sagittal triple inversion-recovery image demonstrates bright signal intensity in most parts of mass (arrow).
C. Postcontrast double inversion-recovery image demonstrates hyperenhancement of mass (arrow).
D. Gross specimen demonstrates yellow soft tissue mass with narrow base of attachment (arrow) to right ventricle.

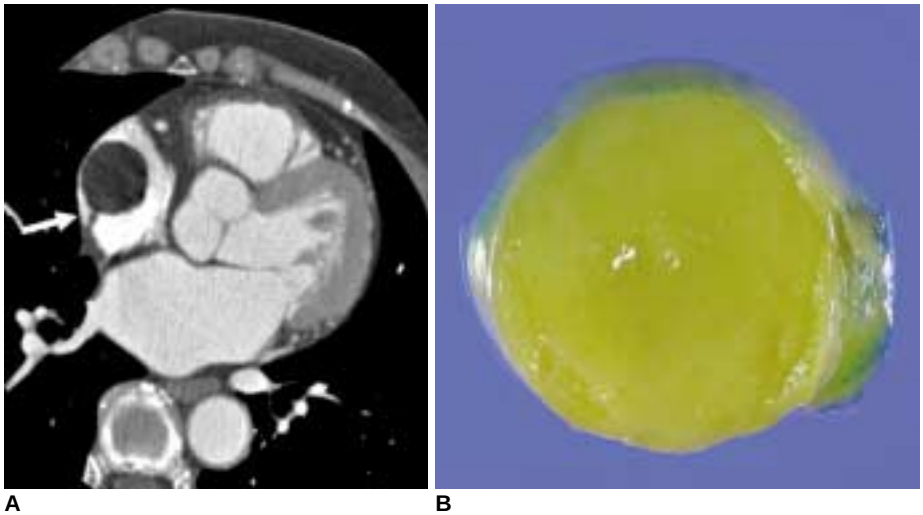

A B

Fig. 4. Right atrial lipoma in 62-year-old female.
A. ECG-gated multidetector CT image shows homogeneously low-attenuated mass with pedicle (arrow) attached to free wall of right atrium.
B. Gross specimen with cut section shows fatty nature of mass.

of a contrast material.

Papillary Fibroelastomas

Papillary fibroelastomas are benign endocardial papillomas that mainly affect the cardiac valves and account for approximately 75% of all cardiac valvular tumors (9). Papillary fibroelastomas are usually not observed on CT or MR images as they are small (< 1.5 cm in diameter) and are attached to the moving valves (9). MR imaging typically demonstrates the presence of a mass on a valve leaflet or on the endocardial surface (Fig. 5). These tumors can create turbulence in the blood flow, which might be demonstrated with the use of cine MR imaging.

Fibromas

Fibromas are neoplasms that mainly affect infants and children, being the second most common tumors found in this age group (10). Grossly, the lesions are solid tumors that arise within the myocardium and can grow to a size that obliterates the cavity. The use of CT shows fibromas as homogeneous masses with soft-tissue attenuation, which may be either sharply marginated or infiltrative. Calcification is often observed (Fig. 6A) (10). These tumors are normally homogeneously isointense to hypointense relative to the myocardium as seen on T1- and T2-weighted images due to a dense, fibrous nature. For the same reason, these tumors often show delayed enhancement on gadolinium-enhanced MR images (Fig. 6B–D) (11).

Rhabdomyomas

Rhabdomyomas are the most common cardiac tumors in infancy and childhood, and are often associated with tuberous sclerosis in up to 50% of cases (12). Most patients

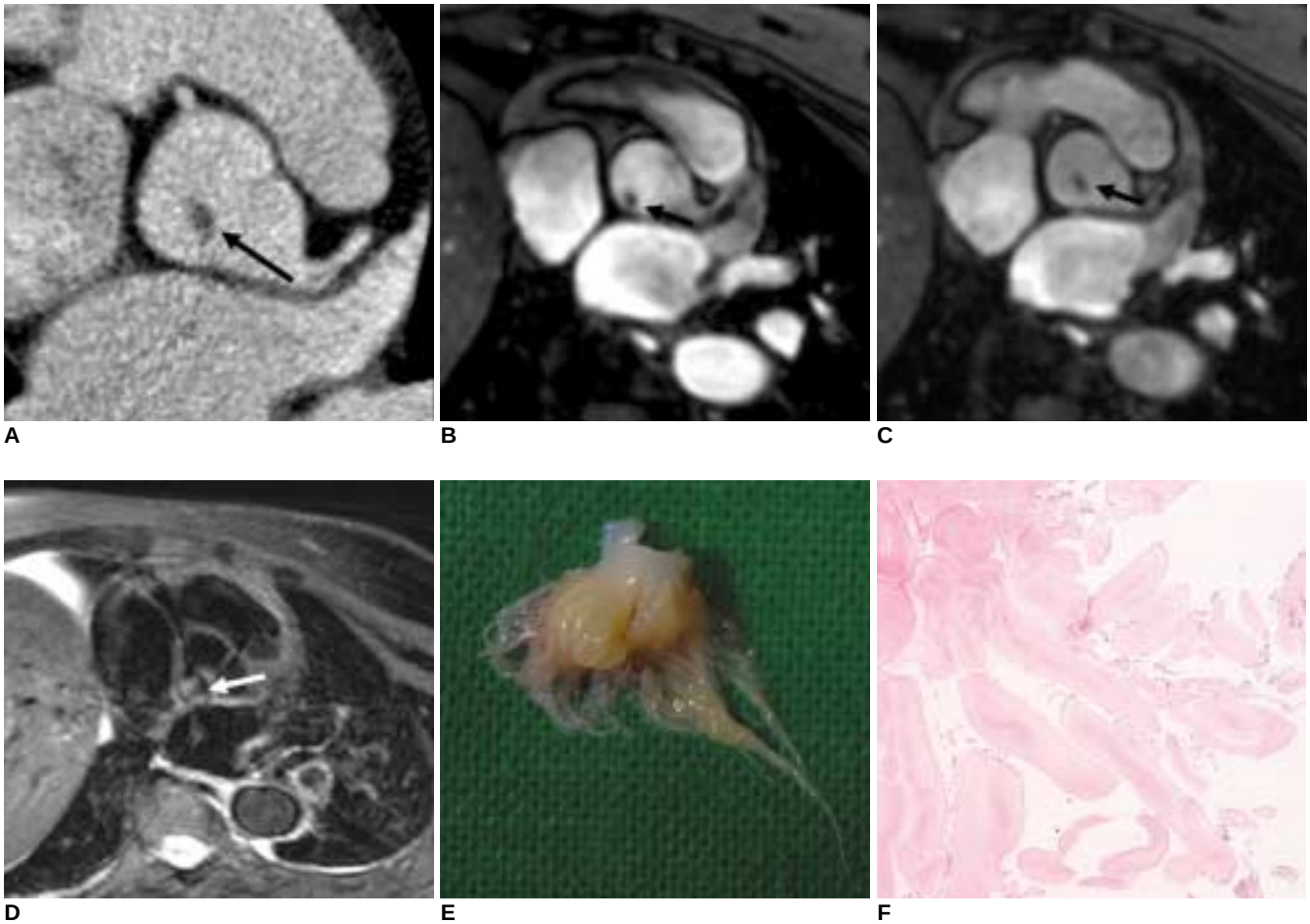

Fig. 5. Papillary fibroelastoma of aortic valve in 60-year-old female.
A. ECG-gated multidetector CT image demonstrates abnormal thickening of aortic valve (arrow).
B, C. Oblique cine MR images demonstrates small mass (arrows) attached to aortic valve that was moving according to valvular motion.
D. Oblique transverse triple inversion-recovery MR image demonstrates slightly high signal intensity of small mass (arrow).
E. Surgical specimen shows small mass with many branching frond-like structures.
F. Photomicrograph (Hematoxylin & Eosin staining, ×150) shows fibrous core and scattered smooth muscle cells within papillary projections.

are asymptomatic, and rhabdomyomas generally regress spontaneously. These tumors originate within the myocardium, typically in the ventricles, and multiple lesions may be present in up to 90% of cases (12). Rhabdomyomas appear isointense to marginally hyperintense as compared with the myocardium as seen on T1-

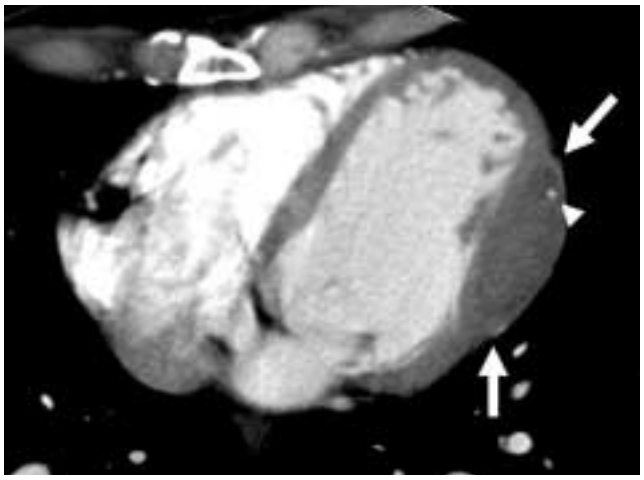

Fig. 6. Left ventricular fibroma in 48-year-old female.
A. ECG-gated multidetector CT image shows myocardial thickening (arrows) and spotty calcification (arrowhead) in lateral wall of left ventricle.
B. Transverse double inversion-recovery MR image shows hypointense mass (arrows) in myocardium of left ventricle.
C. Transverse triple inversion-recovery MR image also shows hypointense mass (arrows) in myocardium of left ventricle.
D. Delayed MR image with suppression of normal myocardial signal 10 minutes after administration of gadolinium demonstrates hyperenhancement of mass (arrows).

A

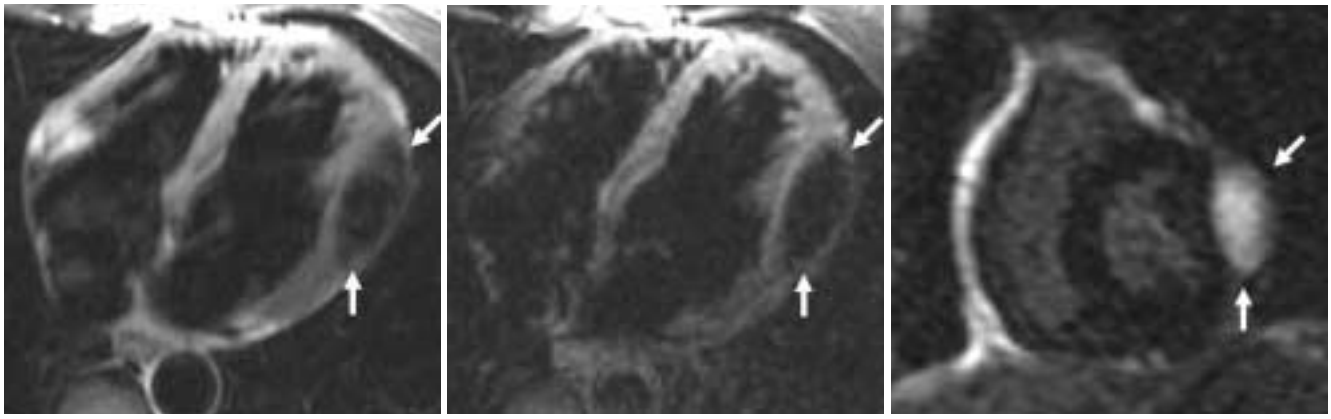

B C D

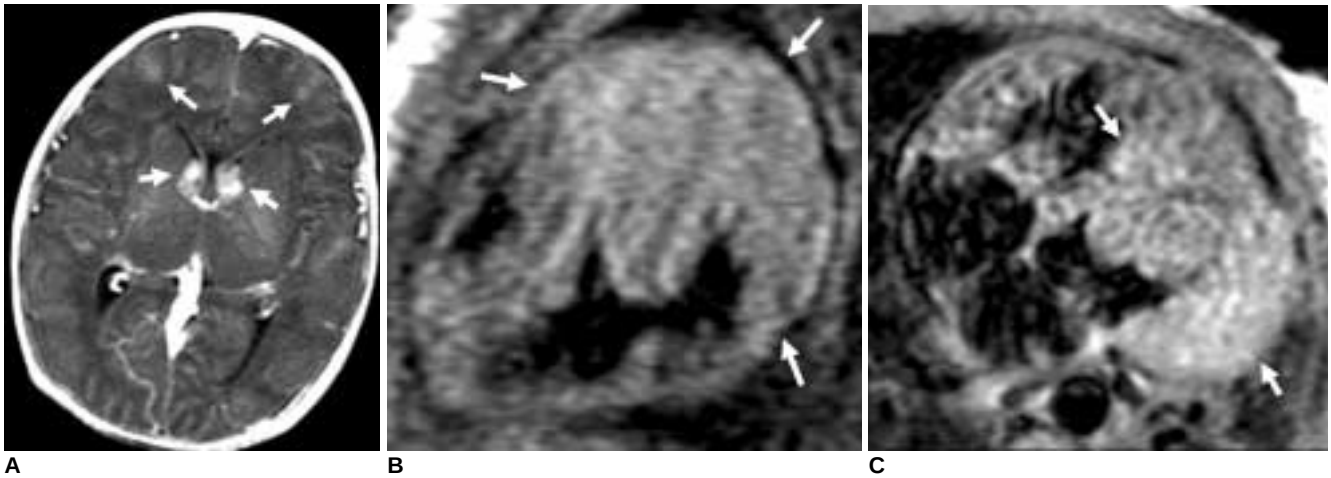

A B C

Fig. 7. Cardiac rhabdomyoma in newborn with tuberous sclerosis.
A. Gadolinium-enhanced T1-weighted MR image shows abnormal enhancing lesions (arrows) in both caudate nuclei and frontal lobes, indicating presence of tubers.
B. Sagittal T1-weighted spin echo MR image shows isointense mass (arrows) in septum and anterior wall of left ventricle.
C. Transverse gadolinium-enhanced T1-weighted spin echo MR image shows mild enhancement of mass (arrows).

weighted images and hyperintense as seen on T2-weighted images (Fig. 7).

Hemangiomas

Hemangiomas are benign vascular tumors that comprise approximately 5–10% of benign tumors (5). Cardiac hemangiomas are heterogeneous as depicted on pre-contrast CT images and are intensely enhanced as seen on CT images obtained after the administration of a contrast material. As with hepatic hemangiomas, these tumors typically show intermediate signal intensity as seen on T1-weighted images and become hyperintense as seen on the T2-weighted images (Fig. 8) (13).

PRIMARY MALIGNANCIES

Angiosarcomas

The most common cardiac sarcomas are angiosarcomas that comprise 37% of all cases (5). These lesions are malignant mesenchymal tumors and usually cause right-sided heart failure or tamponade as the tumors tend to occur in the right atrium and involve the pericardium. Presentation is late, and there is often the presence of metastases at the time of diagnosis, particularly to the lung.

Invasive behavior is a feature of malignant lesions with pericardial or pleural effusion. The use of CT often shows the presence of a low-attenuated mass in the right atrium, which might be irregular or nodular (Fig. 9). Cardiac sarcomas may have heterogeneous signal intensity as seen on MR images (Fig. 9), with areas of high signal intensity as seen on T2-weighted images representing the blood-filled spaces within the neoplasm. A papillary appearance can be observed as a specific MR feature of an angiosarcoma, with a nodular area of high signal intensity interspersed within areas of intermediate signal intensity as seen on T1- and T2-weighted images (14). In cases with diffuse pericardial infiltration, some investigators have described linear enhancement along the vascular spaces as a "sunray"

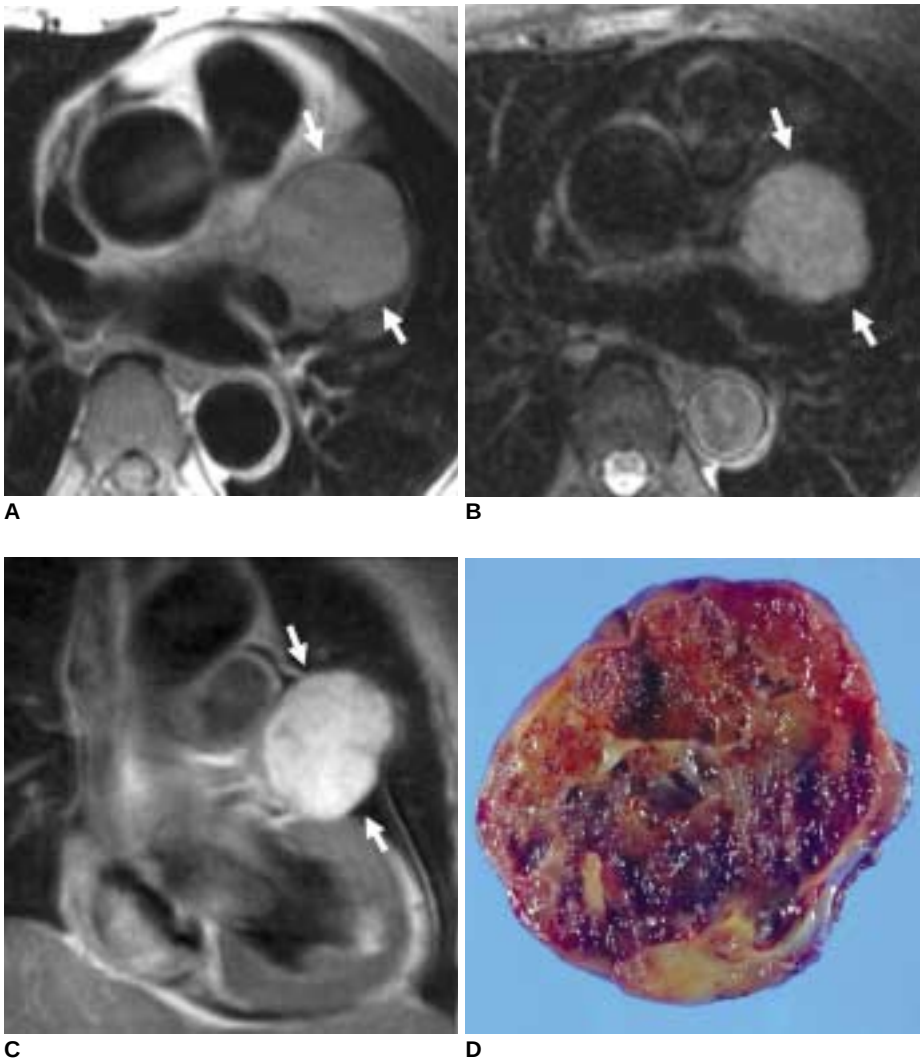

Fig. 8. Cavernous hemangioma of left atrial appendage in 66-year-old female.
A. Transverse double inversion-recovery MR image shows intermediate signal intensity mass (arrows) in left atrial appendage.
B. Transverse triple inversion-recovery MR image shows hyperintense mass (arrows) with smooth margin.
C. Coronal gadolinium-enhanced double inversion-recovery MR image shows strong enhancement of lesion (arrows).
D. Gross specimen with cut section demonstrates trabecular, hemorrhagic, and cystic appearance of mass.

appearance (14).

Other Cardiac Sarcomas

Although angiosarcomas are the most common cardiac sarcomas, all types of sarcomas, including undifferentiated sarcomas, malignant fibrous histiocytomas (MFHs), leiomyosarcomas, osteosarcomas, lymphosarcomas, myxosarcomas, neurogenic sarcomas, synovial sarcomas, neurofibrosarcomas, and Kaposi's sarcomas can affect the heart. Although most angiosarcomas occur in the right atrium, the other sarcomas affect the left atrium more frequently, which is an important differentiating feature (5).

Malignant fibrous histiocytomas consist of primitive mesenchymal, fibroblastic, and histiocytic cells arranged in a storiform pattern (15). The most common location of the MFHs is the left atrium where the tumors are usually attached to the posterior wall (Fig. 10) (15). Distinguishing MFHs from a benign cardiac tumor might be difficult on a clinical and imaging basis. MR imaging demonstrates the presence of a MFH as a mass with a nonspecific signal intensity as seen on T1- and T2-weighted images. A MFH arises from the posterior wall of the left atrium and can extend into the pulmonary veins (Fig. 10). This finding would not normally be expected with a myxoma.

Myxosarcoma is a rare form of primary malignant tumors that is very difficult to differentiate from a myxoma (Fig. 11). The ratio between the incidence of myxomas and myxosarcomas is approximately 100: 0.8 and the prognoses of the two tumor types are very different (16). Myxosarcomas have local recurrences, involving the pulmonary artery, pericardium or pleura and distant metastases, with the brain being the site most affected (16).

Primary Cardiac Lymphomas

Primary cardiac lymphomas are extremely rare, with a reported incidence of 0.15 to 1% (1, 5). A diffuse large B cell lymphoma is the most common type of primary cardiac lymphoma encountered. Most cases of cardiac lymphomas are solid, infiltrative tumors in one or multiple chambers of the heart. The massive infiltration of lymphoma cells in the myocardium results in irregular thickening of the walls of the heart, mimicking classic hypertrophic cardiomyopathy (HCM) (1, 5). CT images show cardiac lymphomas as hypo- or iso-attenuated infiltrative soft tissue masses as compared with the myocardium, and the masses demonstrate heterogeneous enhancement after the administration of a contrast agent (17). With the use of MR imaging, these tumors appear

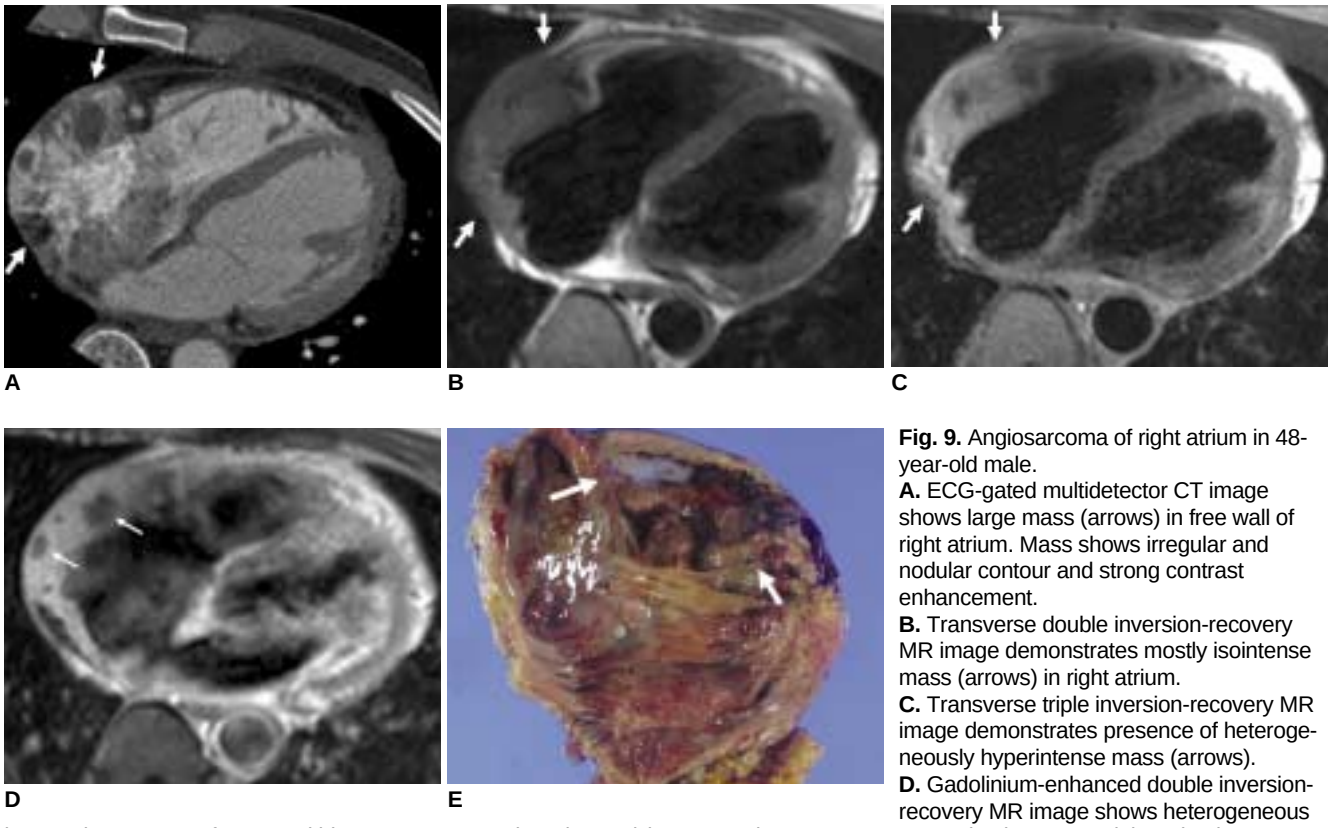

Fig. 9. Angiosarcoma of right atrium in 48-year-old male.
A. ECG-gated multidetector CT image shows large mass (arrows) in free wall of right atrium. Mass shows irregular and nodular contour and strong contrast enhancement.
B. Transverse double inversion-recovery MR image demonstrates mostly isointense mass (arrows) in right atrium.
C. Transverse triple inversion-recovery MR image demonstrates presence of heterogeneously hyperintense mass (arrows).
D. Gadolinium-enhanced double inversion-recovery MR image shows heterogeneous hyperenhancement of mass. Within mass, some portions (arrows) have no enhancement, representing intratumoral thrombosis.
E. Gross specimen shows irregular mass (arrows) of right atrium. Mass had multiple intratumoral thrombi.

isointense as seen on T1-weighted images and heterogeneously hyperintense as seen on T2-weighted images. The tumors demonstrate heterogeneous enhancement after the administration of a gadolinium contrast material, with areas of low enhancement seen in the center of the lesion as compared with the periphery (Fig. 12) (17).

Metastatic Involvement

Metastases to the heart are much more common than primary involvement, with an estimated ratio of 30:1 (18). In the presence of a malignant tumor, cardiac metastases are encountered in 11% of cases (19). The tumors that most frequently metastasize to the heart are lung and breast cancers, melanomas and lymphomas (19).

The epicardium is the site most often affected by metastases (18, 19). Spread is mainly via a retrograde route through the mediastinal lymphatics, leading to implantation in the epicardial surface of the heart. Other tumors such as melanomas and sarcomas usually spread hematogenously to the myocardium and epicardium through the coronary arteries, or less commonly, by the implantation of cancer cells through the vena cava (Fig. 13) (19). Hematogenous metastases in the heart and pericardium are normally accompanied by evidence of hematogenous metastases in other organs. In particular, pulmonary metastases are usually present (19).

Direct extension can occur with thymic, bronchial, breast and esophageal malignancies due to the proximity of the primary lesions to the heart. In addition, transvenous tumor spread relies on an extension of the tumor thrombus into the right atrium through the superior (lung cancers) or inferior vena cava (tumors from the kidney or liver) or an extension into the left atrium via the pulmonary veins. The

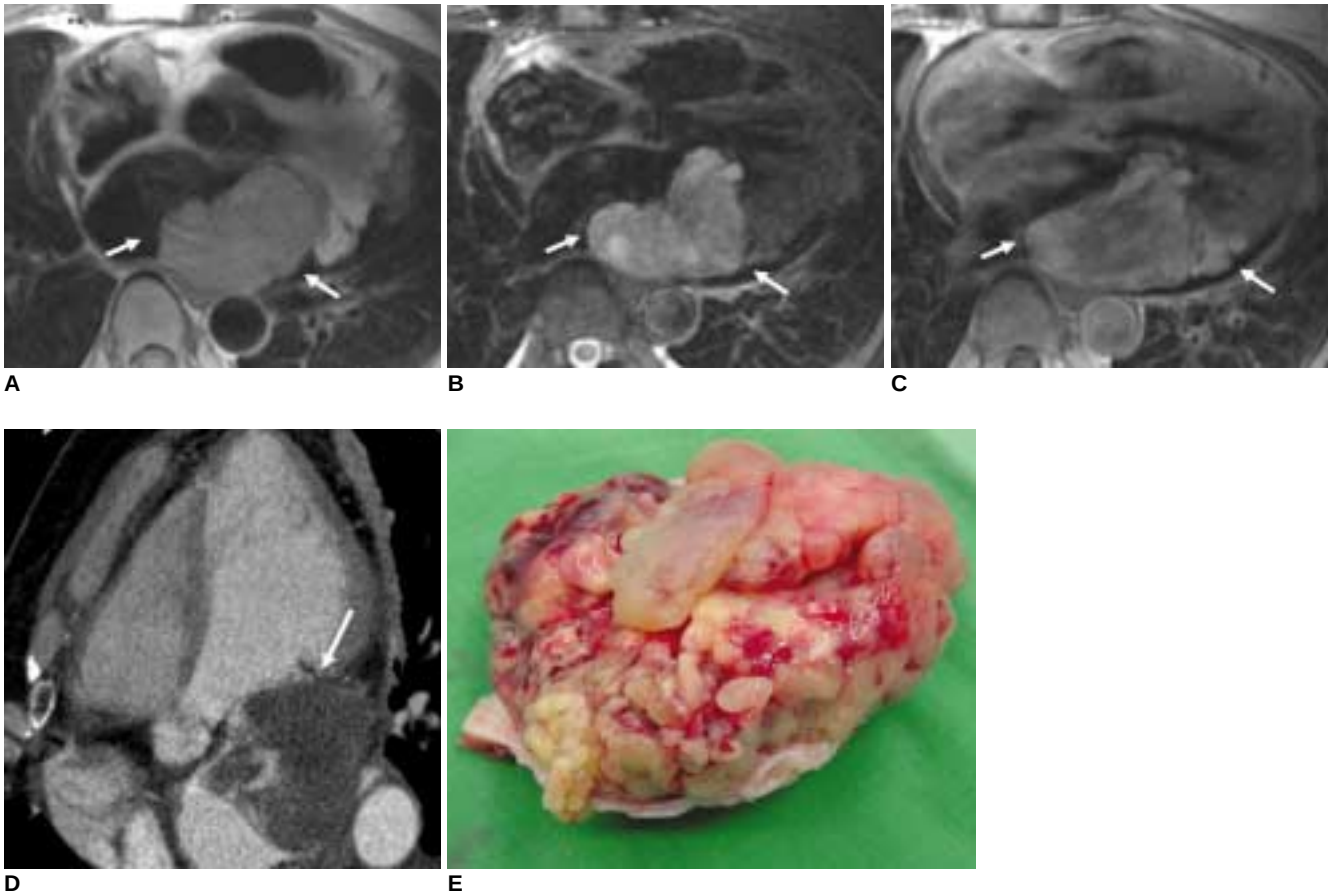

Fig. 10. Malignant fibrous histiocytoma in 57-year-old female.
A. Transverse double inversion-recovery MR image shows large isointense mass (arrows) arising from posterior wall of left atrium that extends into mitral valve.
B. Transverse triple inversion-recovery MR image shows hyperintense mass (arrows) with irregular contour.
C. Gadolinium-enhanced double inversion-recovery MR image shows heterogeneous hyperenhancement of mass (arrows).
D. ECG-gated multidetector CT reformatted image shows that mitral valve (arrow) is abutting mass. At surgery, mitral valve was found to be involved by malignant mass. Mass was removed and mitral valve was replaced with artificial valve.
E. Gross specimen shows presence of multilobulated mass. Cut surface was seen with heterogeneous, gelatinous, myxoid, yellowish white and hemorrhagic appearance (not shown).

enhancement patterns after the administration of gadolinium might be helpful to differentiate a thrombus from a combined tumor. Tumors would be expected to show heterogeneous enhancement whereas thrombi should not.

Limitations of the Use of Multidetector CT and MRI and Various Pitfalls in the Imaging Evaluation of Cardiac Tumors

The disadvantages of the use of MDCT include radiation exposure to the patient and the need to administer potentially nephrotoxic contrast material. Streak artifacts can occur when the contrast material remains in the right

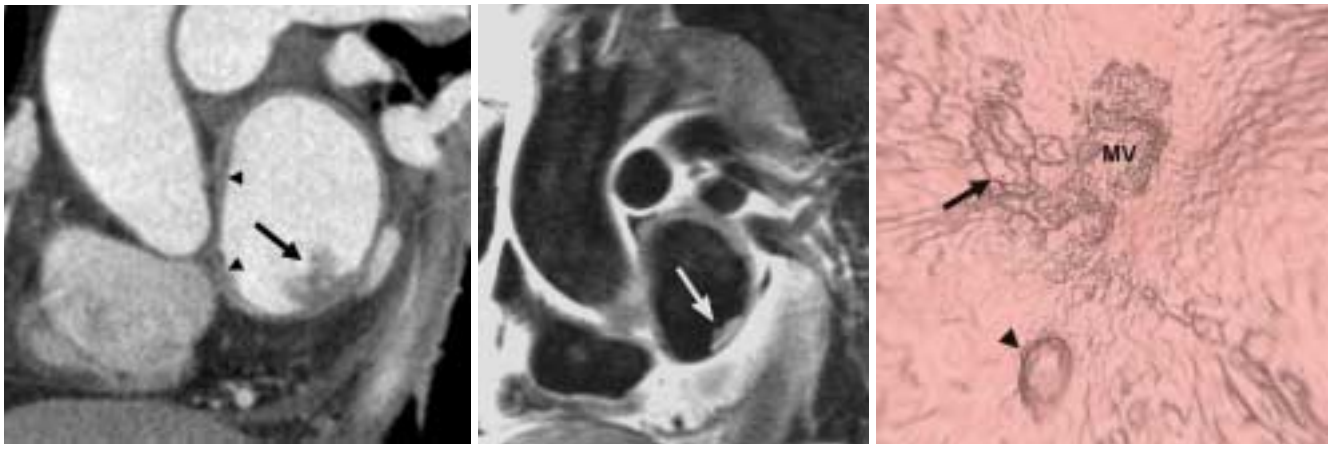

Fig. 11. Left atrial myxosarcoma in 72-year-old female.
A. Reformatted ECG-gated multidetector CT image shows irregular mass (arrow) with broad-base attachment to left atrium. Also, note minimal wall thickening (arrowheads) of interatrial septum due to tumor spread along left atrial wall and septum.
B. Oblique double inversion-recovery MR image depicts hyperintense lesion (arrow) after gadolinium injection.
C. Virtual angioscopic multidetector CT image shows irregular mass (arrow) near mitral valve (MV) and small polypoid mass (arrowhead).
D. At surgery, presence of lobulated soft tissue mass (arrow) and small polypoid lesions were demonstrated (arrowheads).

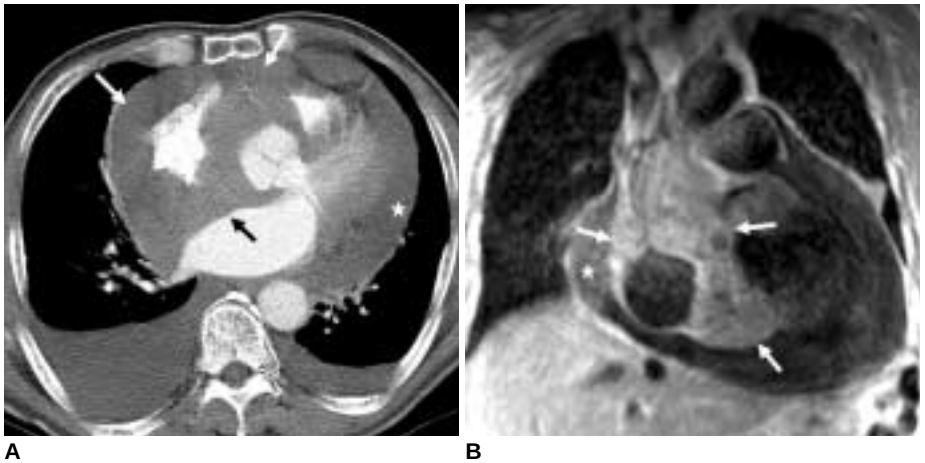

Fig. 12. Primary cardiac lymphoma (diffuse large B-cell type) in 73-year-old male.
A. Non-gated postcontrast multidetector CT image shows homogeneous and mildly hyperattenuated mass (arrows) in right atrial wall and interatrial septum. Mass is spreading along pericardial space. Pericardial effusion (asterisk) is probably due to pericardial invasion.
B. Coronal gadolinium-enhanced double inversion-recovery MR image shows presence of diffuse infiltrative mass (arrows) in right atrium. Mass shows homogeneous enhancement that distinguishes it from pericardial effusion (asterisk).

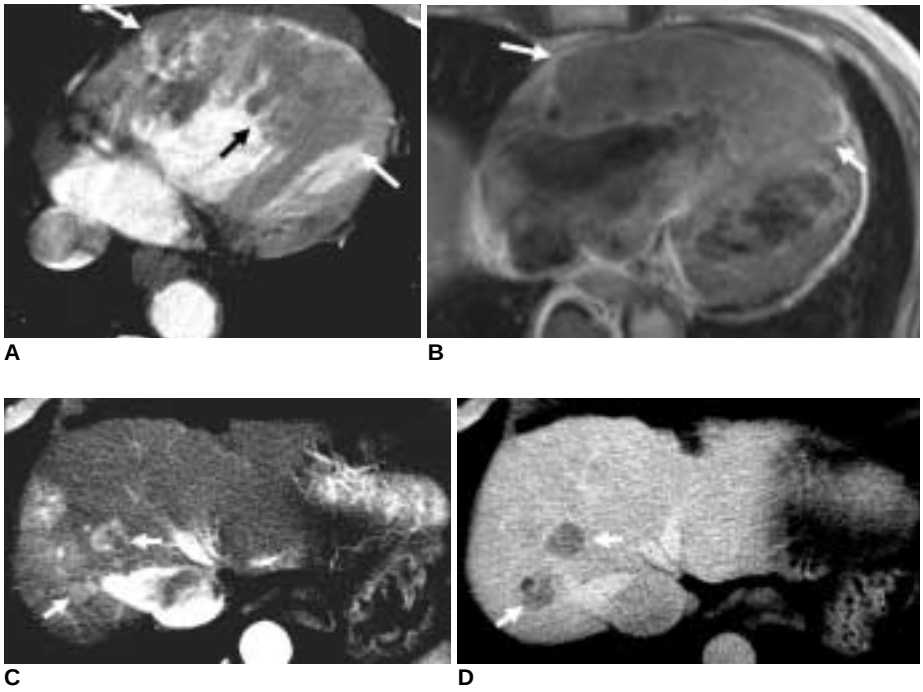

Fig. 13. Hematogenous cardiac metastases from hepatocellular carcinomas in 50-year-old male.
A. ECG-gated multidetector CT image shows marked thickening of right ventricular free wall (arrows).
B. Gadolinium-enhanced transverse double inversion-recovery MR image shows diffuse thickening of right ventricular wall (arrows).
C, D. Arterial (**C**) and delayed (**D**) CT images show multiple hepatocellular carcinomas with characteristic dynamic pattern of early enhancement and wash out (arrows).

heart during image acquisition. In this case, the use of a delayed scan or split-bolus injection (for example, 65 mL at 4 mL/sec followed by 30 mL at 1 mL/sec) or the administration of a contrast-saline mixture (80% and 20%, respectively) instead of an injection of saline only after contrast injection can eliminate streak artifacts and can visualize the right atrial masses. Disadvantages of the use of MRI include a long scan time and the inability to demonstrate calcification and small masses, especially in cardiac valves due to limited spatial resolution (20).

Some benign conditions such as lipomatous hypertrophy, mass-like hypertrophy of the left ventricular myocardium, prominent crista terminalis, and thrombi can mimic a cardiac tumor. Lipomatous hypertrophy of the interatrial septum is a benign condition that is characterized by fat accumulation in the interatrial septum. It results from adipose-cell hyperplasia and is related to advanced age and obesity (21). The tissue appears as a wedge-shape or diffuse septal thickening on CT and MR images with signal intensity comparable to that of subcutaneous fat as seen on T1- and T2-weighed MR images (22). Mass-like hypertrophy of the left ventricular myocardium may mimic cardiac tumors (23). However, mass-like HCM has more homogeneous signal characteristics and perfusion of the lesion is similar to the signal characteristics of the adjacent normal myocardium, except in the areas of fibrosis, whereas tumors often show varying degrees of signal heterogeneity before and after gadolinium administration. In addition, HCM will show variable degrees of contractility whereas a true mass will have no contractile portion (23). The line of union between the right atrium and the right auricle is present on the interior of the atrium in the form of a vertical crest, known as the crista terminalis. Regression of the crista terminalis is known to occur to variable degrees; thus, widely variable prominence exhibited by this structure is seen (24, 25). A prominent crista terminalis can be misinterpreted as a right atrial mass, especially when echocardiography is used as an isolated imaging technique for the heart. MRI will prevent misinterpretation of the presence of normal intracardiac structures by the accurate identification of the exact position and extension of fibromuscular prominent structures to distinguish the structures from a neoplasm or thrombus (25). A thrombus is most likely to be located posterior in the left atrium. The signal intensity characteristics of a thrombus vary with MR imaging and are dependent on the age of the thrombus. An acute thrombus will appear bright as seen on both T1- and T2-weighted MR images, whereas a subacute thrombus will appear bright as seen on T1-weighted images with hypointense areas seen on T2-weighted images due to the paramagnetic effects of methemoglobin and shortening of the T2 relaxation times. A chronic organized thrombus will exhibit hypointensity as seen on both T1- and T2-weighted images due to a depleted water content (20). Gadolinium contrast material is also useful in differentiating a thrombus from a tumor, as the thrombus should not show enhancement whereas a tumor usually shows enhancement (26). However, an organized thrombus may show some surface enhancement.

CONCLUSION

Multidetector CT and MRI may be useful in the differentiation of benign and malignant cardiac masses. MDCT is useful for the evaluation of calcification and fat content within a mass and the high spatial resolution of MDCT is beneficial to define small lesions. MDCT is useful in the staging of malignant tumors. The excellent contrast resolution with the use of MRI allows characterization of fibromas and hemangiomas. Homogeneity of a mass due to compact cellularity may be characteristic of a lymphoma. Acquisition of postcontrast sequences enables better depiction of tumor vascularity and can be used to define tumor borders. MRI has an important role in differentiating thrombi from cardiac tumors. Besides the characteristics of a tumor, a preoperative imaging assessment of cardiac tumors using MDCT and MRI might help determine resectability of a tumor and allow planning for reconstruction of the cardiac chambers.

References

1. Sutsch G, Jenni R, von Segesser L, Schneider J. Heart tumors: incidence, distribution, diagnosis. Exemplified by 20,305 echocardiographies. *Schweiz Med Wochenschr* 1991;121:621-629
2. McAllister HA Jr, Fenoglio JJ Jr. *Tumors of the cardiovascular system*. In: *Atlas of tumor pathology*, 2nd ed. Washington, DC: Armed Forces Institute of Pathology, 1978:15
3. Araoz PA, Eklund HE, Welch TJ, Breen JF. CT and MR imaging of primary cardiac malignancies. *Radiographics* 1999;19:1421-1434
4. Hong C, Becker CR, Huber A, Schoepf UJ, Ohnesorge B, Knez A, et al. ECG-gated reconstructed multi-detector row CT coronary angiography: effect of varying trigger delay on image quality. *Radiology* 2001;220:712-717
5. Burke A, Virmani R. *Tumors of the heart and great vessels.* In: *Atlas of tumor pathology*, 3rd ed. Washington, DC: Armed Forces Institute of Pathology, 1996:79-90
6. Moriyama Y, Saigenji H, Shimokawa S, Toyohira H, Taira A. The surgical treatment of 30 patients with cardiac myxomas: a comparison of clinical features according to morphological classification. *Surg Today* 1994;24:596-598
7. Grebenc ML, Rosado-de-Christenson ML, Green CE, Burke AP, Galvin JR. Cardiac myxoma: imaging features in 83 patients. *Radiographics* 2002;22:673-689
8. Masui T, Takahashi M, Miura K, Naito M, Tawarahara K. Cardiac myxoma: identification of intratumoral hemorrhage and calcification on MR images. *AJR Am J Roentgenol* 1995;164:850-852
9. Edwards FH, Hale D, Cohen A, Thompson L, Pezzella AT, Virmani R. Primary cardiac valve tumors. *Ann Thorac Surg* 1991;52:1127-1131
10. Burke AP, Rosado-de-Christenson M, Templeton PA, Virmani R. Cardiac fibroma: clinicopathologic correlates and surgical treatment. *J Thorac Cardiovasc Surg* 1994;108:862-870
11. De Cobelli F, Esposito A, Mellone R, Papa M, Varisco T, Besana R, et al. Images in cardiovascular medicine. Late enhancement of a left ventricular cardiac fibroma assessed with gadolinium-enhanced cardiovascular magnetic resonance. *Circulation* 2005;112:E242-E243
12. Webb DW, Thomas RD, Osborne JP. Cardiac rhabdomyomas and their association with tuberous sclerosis. *Arch Dis Child* 1993;68:367-370
13. Newell JD 2nd, Eckel C, Davis M, Tadros NB. MR appearance of an arteriovenous hemangioma of the interventricular septum. *Cardiovasc Intervent Radiol* 1988;11:319-321
14. Yahata S, Endo T, Honma H, Ino T, Hayakawa H, Ogawa M, et al. Sunray appearance on enhanced magnetic resonance image of cardiac angiosarcoma with pericardial obliteration. *Am Heart J* 1994;127:468-471
15. Okamoto K, Kato S, Katsuki S, Wada Y, Toyozumi Y, Morimatsu M, et al. Malignant fibrous histiocytoma of the heart: case report and review of 46 cases in the literature. *Intern Med* 2001;40:1222-1226
16. Awamleh P, Alberca MT, Gamallo C, Enrech S, Sarraj A. Left atrium myxosarcoma: an exceptional cardiac malignant primary tumor. *Clin Cardiol* 2007;30:306-308
17. Dorsay TA, Ho VB, Rovira MJ, Armstrong MA, Brissette MD. Primary cardiac lymphoma: CT and MR findings. *J Comput Assist Tomogr* 1993;17:978-981
18. Lam KY, Dickens P, Chan AC. Tumors of the heart. A 20-year experience with a review of 12,485 consecutive autopsies. *Arch Pathol Lab Med* 1993;117:1027-1031
19. Klatt EC, Heitz DR. Cardiac metastases. *Cancer* 1990;65:1456-1459
20. Sparrow PJ, Kurian JB, Jones TR, Sivananthan MU. MR imaging of cardiac tumors. *Radiographics* 2005;25:1255-1276
21. Gaerte SC, Meyer CA, Winer-Muram HT, Tarver RD, Conces DJ Jr. Fat-containing lesions of the chest. *Radiographics* 2002;22:S61-S78
22. Hoffmann U, Globits S, Frank H. Cardiac and paracardiac masses. Current opinion on diagnostic evaluation by magnetic resonance imaging. *Eur Heart J* 1998;19:553-563
23. Hansen MW, Merchant N. MRI of hypertrophic cardiomyopathy: part I, MRI appearances. *AJR Am J Roentgenol* 2007;189:1335-1343
24. Mirowitz SA, Gutierrez FR. Fibromuscular elements of the right atrium: pseudomass at MR imaging. *Radiology* 1992;182:231-233
25. Gaudio C, Di Michele S, Cera M, Nguyen BL, Pannarale G, Alessandri N. Prominent crista terminalis mimicking a right atrial mixoma: cardiac magnetic resonance aspects. *Eur Rev Med Pharmacol Sci* 2004;8:165-168
26. Paydarfar D, Krieger D, Dib N, Blair RH, Pastore JO, Stetz JJ Jr, et al. In vivo magnetic resonance imaging and surgical histopathology of intracardiac masses: distinct features of subacute thrombi. *Cardiology* 2001;95:40-47